Supporting Information

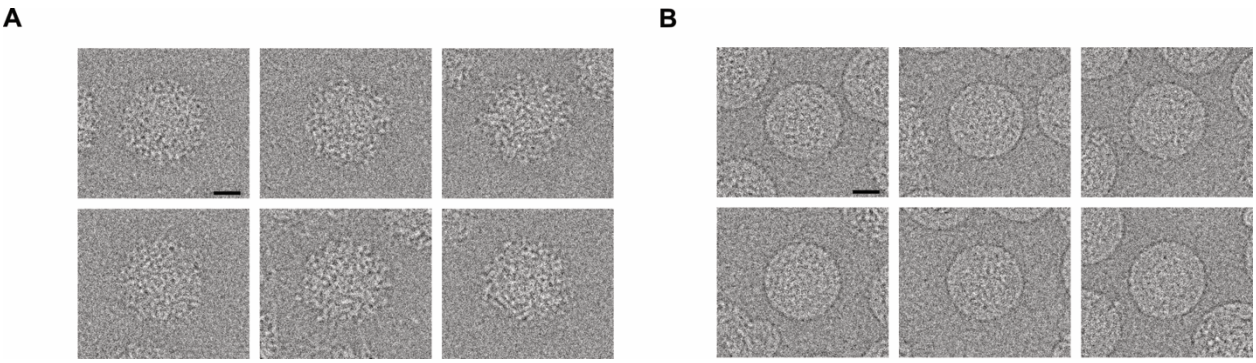

Figure S1. Cryo-EM of immature and mature KUNV. Particles from cryo-electron micrographs of (*A*) immature "spiky" KUNV and (*B*) mature "smooth" KUNV. The defocus for these particles was 2-3 μm. Scale bar is 200 Å.

A

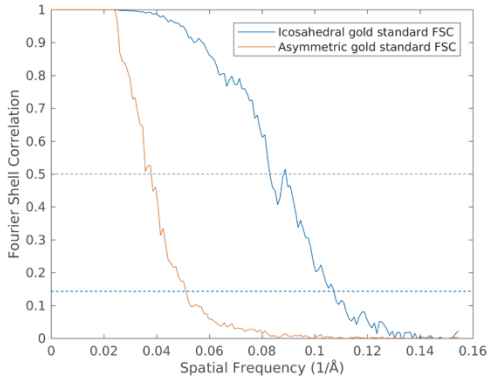
Icosahedral gold standard FSC
Asymmetric gold standard FSC
Fourier Shell Correlation
Spatial Frequency (1/Å)
1
0.9
0.8
0.7
0.6
0.5
0.4
0.3
0.2
0.1
0
0 0.02 0.04 0.06 0.08 0.1 0.12 0.14 0.16

B

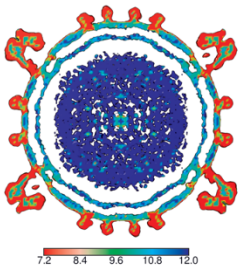
7.2 8.4 9.6 10.8 12.0

C

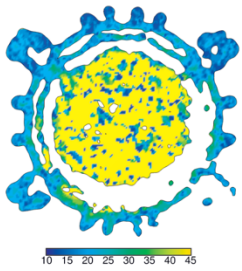
10 15 20 25 30 35 40 45

D

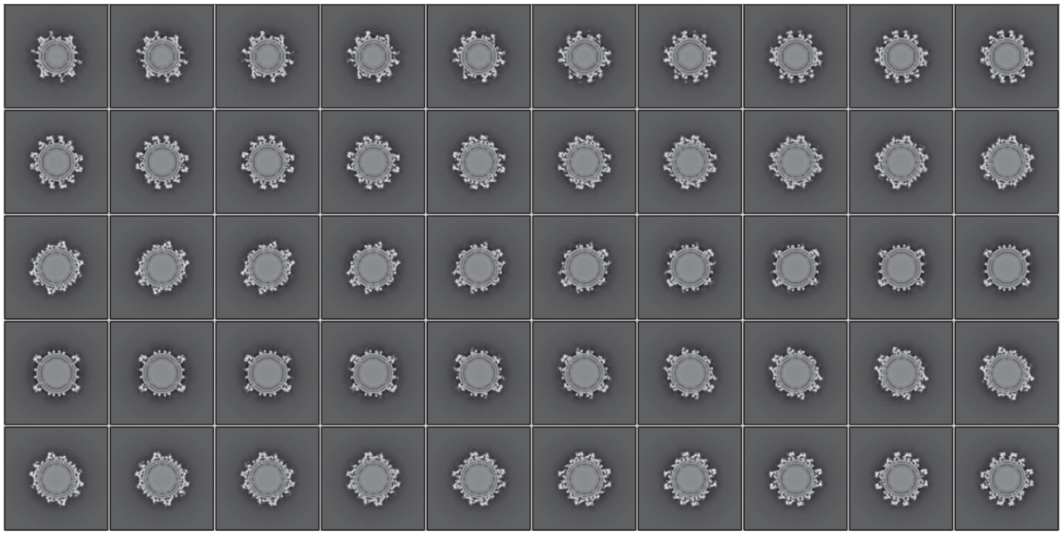

E

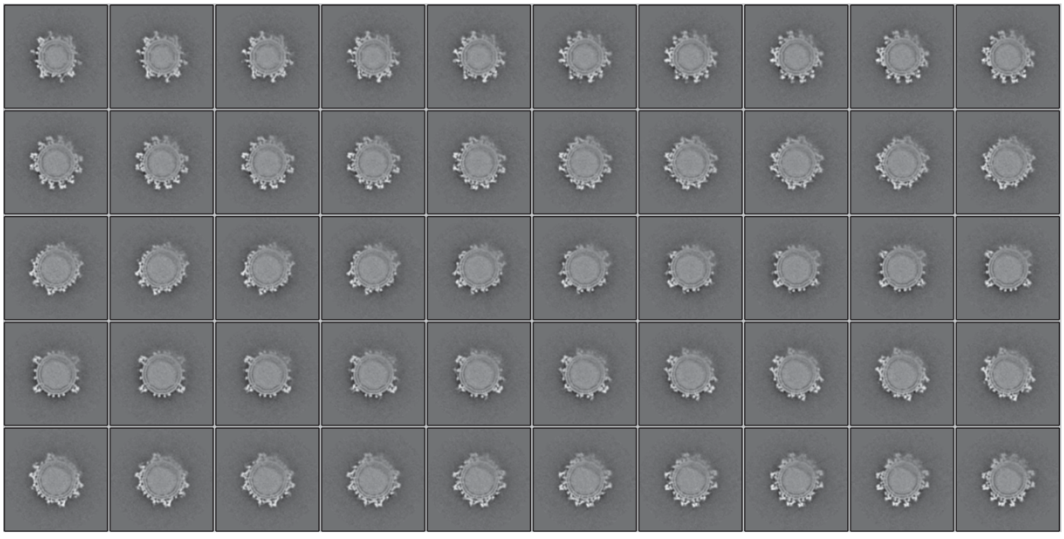

Figure S2. Characterization of immature KUNV reconstructions. (*A*) FSC curves of two random half-sets of icosahedral (blue) and asymmetric (red) reconstructions. (*B*) Central cross-section of the icosahedral reconstruction colored by local resolution. (*C*) Central cross-section of the asymmetric reconstruction colored by local resolution. Grayscale sections of (*D*) icosahedral and (*E*) asymmetric reconstructions.

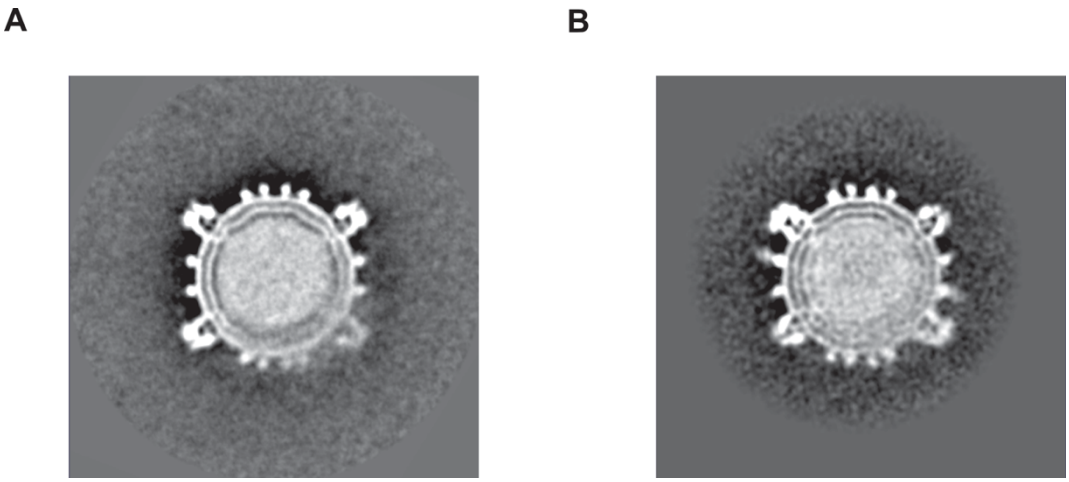

Figure S3. Asymmetric reconstructions of flaviviruses. (*A*) Grayscale central section of the immature KUNV reconstruction. (*B*) Grayscale central section of the immature ZIKV reconstruction.

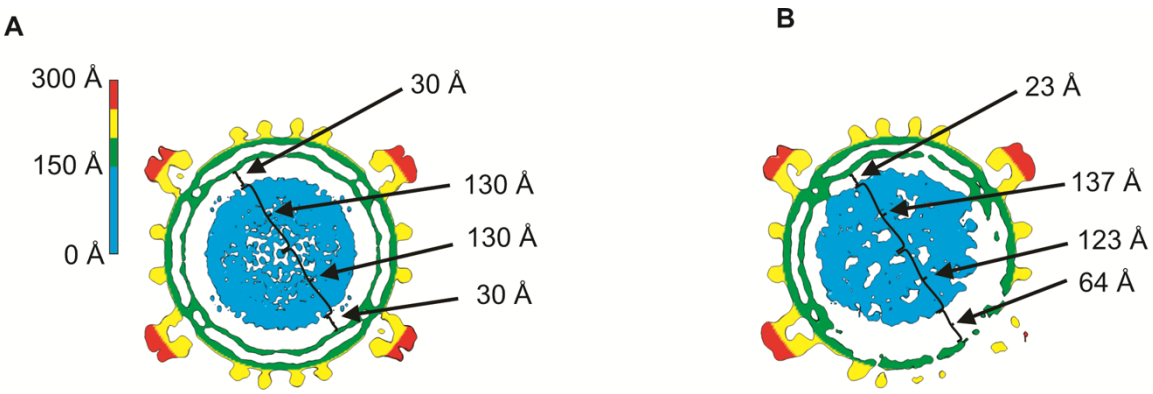

Figure S4. Measurements of immature KUNV. (*A*) Central cross-section of the icosahedral reconstruction colored radially as indicated in color key. (*B*) Central cross-section of the asymmetric reconstruction. Reconstructions are contoured at 3 σ, and arrows indicate distances defined by brackets.

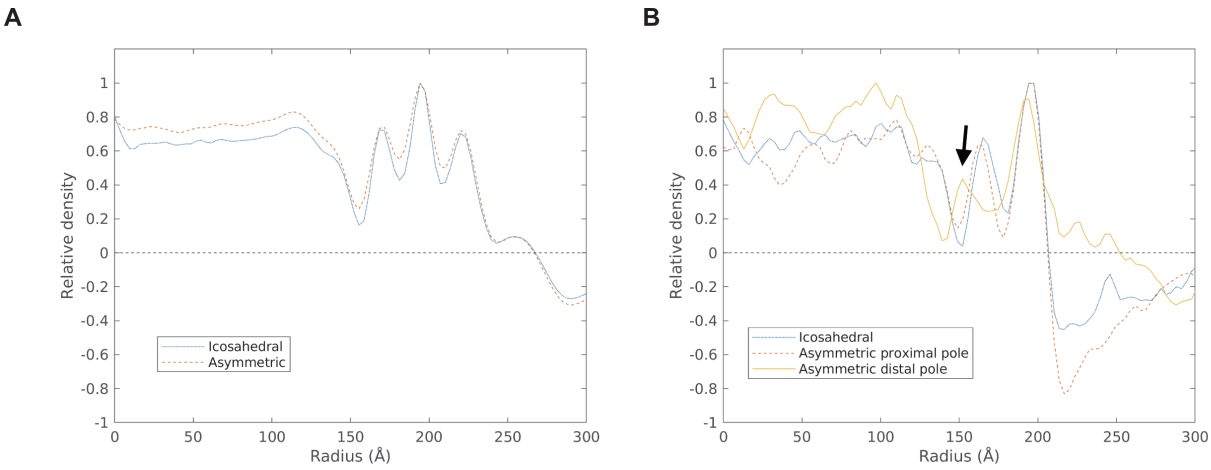

Figure S5. Comparison of electron density in immature KUNV reconstructions. (*A*) Radial density plot of rotationally averaged icosahedral and asymmetric reconstructions. The center of the asymmetric reconstruction was defined by aligning the reconstruction to the icosahedral reconstruction. The icosahedral and asymmetric reconstructions are shown in blue and red, respectively. (*B*) Radial density plots calculated in the direction of a 5-fold axis. The icosahedral reconstruction was rotated so that a 5-fold axis was positioned along the Z-axis in Chimera. The asymmetric reconstruction was aligned to the icosahedral reconstruction, by aligning the 5-fold axis closest to either the proximal pole or distal pole to the icosahedral 5-fold axis positioned on the Z-axis. The icosahedral radial density plot is shown in blue, and asymmetric radial density plots for the proximal pole and distal pole are shown in red and yellow, respectively. The asymmetric distal and proximal pole share density features such as a peak at ~195 Å for the outer leaflet of the membrane. However, the asymmetric distal pole has a distinct density distribution, such as the peak at ~150 Å (black arrow) that is not observed in the icosahedral reconstruction or at the proximal pole of the asymmetric reconstruction.

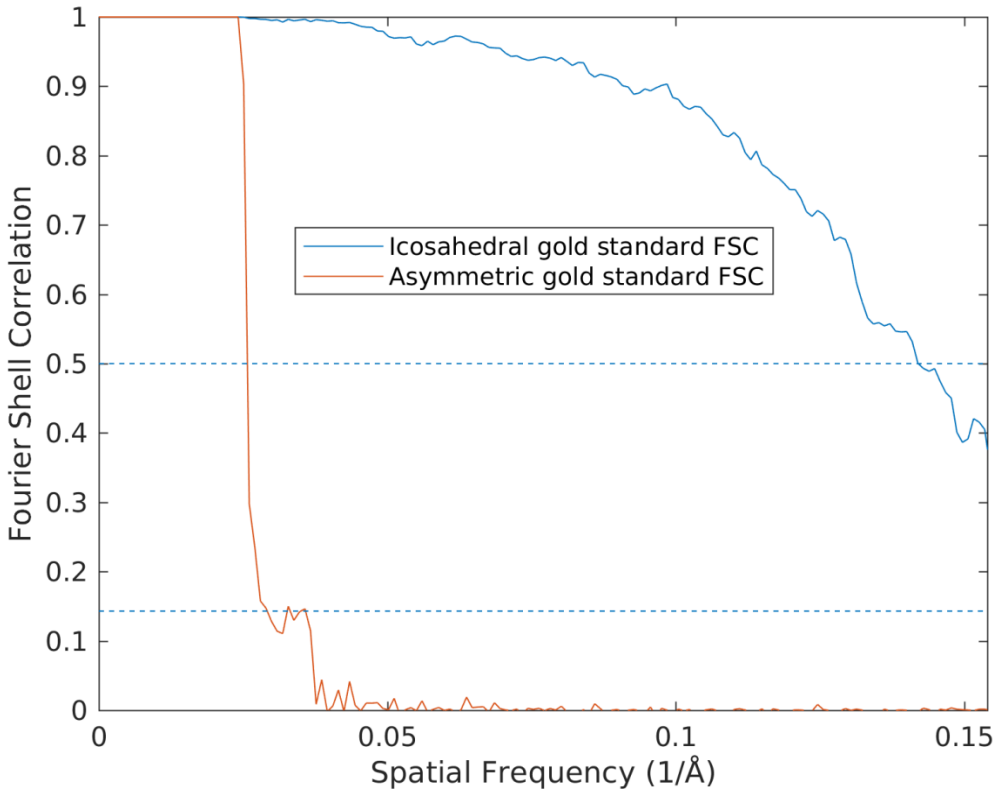

Fig S6. Resolution of mature KUNV reconstructions. FSC curves of two random halfsets of the icosahedral (blue) and asymmetric (red) reconstructions. The icosahedral reconstruction reached the Nyquist frequency at a pixel size of 3.24 Å/pixel (4x binned).

Table S1. Cryo-EM data collection and processing statistics.

Dataset	Immature KUNV	Mature KUNV
Microscope	Titan Krios	Titan Krios
Accelerating voltage, kV	300	300
Camera	Gatan K2 Summit	Gatan K2 Summit
Mode	Super-resolution	Super-resolution
Number of movies	387	369
Pixel size, Å/pixel	0.81	0.81
Dose rate, e^-/pixel/s	8	8
Total dose, $e^-/Å^2$	24	24
Frame rate, ms	200	200
Defocus, µm	0.5-3.0	0.5-3.0
Number of particles for reconstruction	7,396	9,206
Icosahedral resolution, Å	9.3	6.4
Asymmetric resolution, Å	19	35